

# Constraining $\Omega_0$ from X-ray properties of clusters of galaxies at high redshift

R. Sadat<sup>1,2</sup>, A. Blanchard<sup>1</sup>, and J. Oukbir<sup>1,3</sup>

<sup>1</sup> Observatoire Astronomique, 11, rue de l'Université, F-67000 Strasbourg, France

<sup>2</sup> C.R.A.A.G., BP 63, Bouzareah, Algiers, Algeria

<sup>3</sup> D.S.R.I., Juliane Maries Vej 30, DK-2100, Copenhagen, Denmark

Received 2 June 1997 / Accepted 20 August 1997

**Abstract.** Properties of high redshift clusters are a fundamental source of information for cosmology. It has been shown by Oukbir and Blanchard (1997) that the combined knowledge of the redshift distribution of X-ray clusters of galaxies and the luminosity-temperature correlation,  $L_X - T_X$ , provides a powerful test of the mean density of the Universe. In this paper, we address the question of the possible evolution of this relation from an observational point of view and its cosmological significance. We introduce a new indicator in order to measure the evolution of the X-ray luminosity-temperature relation with redshift and take advantage of the recent availability of temperature information for a significant number of high and intermediate redshift X-ray clusters of galaxies. From our analysis, we find a slightly positive evolution in the  $L_X - T_X$  relation. This implies a high value of the density parameter of  $0.85 \pm 0.2$ . However, because the selection of clusters included in our sample is unknown, this can be considered only as a tentative result. A well-controlled X-ray selected survey would provide a more robust answer. XMM will be ideal for such a program.

**Key words:** cosmology: observations – galaxies: clusters – X-rays: galaxies

---

## 1. Introduction

Clusters of galaxies are ideal tools for cosmology since they are the largest “virialized” structures in the Universe. They are strong X-ray emitters, and as such they provide useful information on the evolution and formation of structures in the universe. In particular, cluster evolution can be inferred from the study of X-ray properties of distant clusters. There has been some debates on the existence and the nature of the evolution of X-ray clusters. Oukbir, Blanchard & Bartlett (1997, OBB97 hereafter) established a completely self-consistent modeling of X-ray clusters, and concluded that all the available data can be

reproduced with a much lower rate of evolution than inferred from the EMSS survey (Edge et al., 1990; Henry and Arnaud, 1991, HA91 hereafter). From recent analyses, it seems more and more clear that the X-ray luminosity function evolves (Collins et al., 1997; Nichol et al., 1997; Ebeling et al., 1997), but at a lower rate than has been previously reported.

The Press-Schechter formalism (1974) has been extensively used in order to reproduce the global properties of X-ray clusters (Henry & Arnaud, 1991; Blanchard et al, 1992; Bartlett & Silk, 1993; Colafrancesco & Vittorio, 1994; De Luca et al, 1995 ; Viana & Liddle, 1996; Eke et al, 1996; Kitayama & Suto, 1997; Bahcall et al., 1997; Mathiesen & Evrard, 1997 among others) as this formalism seems to describe accurately the clusters distribution of mass,  $m$ , and redshift,  $z$ . This has also been applied to Sunyaev-Zeldovich number counts (Barbosa et al, 1996). Oukbir & Blanchard (1992) showed that the existence of high temperature clusters at high redshift is more likely in open universes than in a universe with the critical density. Oukbir & Blanchard (1997, OB97 hereafter) showed that the relative evolution of cluster abundance depends only on the growth rate of structure, which depends on the cosmological parameters of universe, but not on the spectrum of the primordial fluctuations. On this basis, they have proposed a new test for constraining  $(\Omega_0, \Lambda)$ : the redshift evolution of the X-ray cluster temperature distribution function.

Such a test requiring the knowledge of the evolution of the temperature distribution function is difficult to apply. Henry (1997) has shown a first application, while Donahue et al. (1997) have presented similar considerations. Carlberg et al. (1997), C97 hereafter, present a tentative application of this test on the basis of velocity dispersion. Bahcall et al. (1997) also present an application of this test. However, by fitting the evolution of the luminosity-temperature relation in order to match the redshift distribution of EMSS clusters, OB97 showed that knowledge of the evolution of this quantity allows an equivalent determination of  $\Omega_0$  in an efficient way. Few attempts have been made to measure the evolution of the  $L_X - T_X$  relation and it has not yet been applied to constrain cosmological parameters. In this

---

Send offprint requests to: R. Sadat

paper we attempt for the first time a comparison of the theoretical predictions of the  $L_X - T_X$  relation with available data we have gleaned from the literature. In Sect. 2, we briefly discuss the foundations of this test. In Sect. 3 we discuss the set of clusters we have used to perform the test. In Sect. 4, we describe the method we have used to estimate the possible evolution.

## 2. Clusters properties and the mean density of the universe

The Press-Schechter (1974) formalism seems to give an accurate determination of the mass function. The reason for this has been a matter of debate, but it has allowed investigation of the non-linear evolution of structure formation in much detail. This has been widely used to put constraints on cosmological parameters, such as the amplitude and the shape of the power spectrum on galaxy clusters scales by comparison with observations. However, cluster masses are not directly measured, therefore it is necessary to establish relations between the mass and “observables” such as the X-ray luminosity or the X-ray temperature. As the luminosity of a cluster is difficult to relate to its virial mass from theoretical arguments, it has been argued by some authors that the temperature distribution function is more adequate for a fruitful comparison, although Balland & Blanchard (1997) showed that hydrostatic equilibrium does not provide a one-to-one correspondence between mass and temperature. This relation should therefore be taken from the numerical simulations where gas dynamics are taken into account (Evrard, Metzler & Navarro 1996). The consequence for cosmology of the observed X-ray luminosity and X-ray temperature distribution functions has been investigated in recent years. OBB97 have shown that a comprehensive description can be constructed, in a consistent way, provided that the relation between luminosity and temperature is specified (from the observations). Such a scheme has been used by OB97 to investigate the cosmological implication of X-ray clusters in an open cosmology and to establish a self-consistent modeling in such a context. They have shown that although the properties of X-ray clusters at redshift zero can be well reproduced in an open model, the redshift evolution is significantly different: this is due to the fact that in open model universes the growth rate of fluctuations is lower than in a Einstein-de Sitter universe. Therefore, at high redshift, a higher number density is expected than in an  $\Omega_0 = 1$  universe. Specifically, they prove (see their Sect. 4) that the redshift evolution of the number of clusters of a given mass, or equivalently of a given apparent temperature, is almost independent of the spectrum of the primordial fluctuations, but that it depends on the mean density of the universe (and on others cosmological parameters of the universe). The evolution of the mass function therefore allows one to measure the mean density of the universe (and the cosmological constant), providing a new cosmological test, based on the dynamics of the universe as a whole.

**Table 1.** Temperatures and bolometric luminosities for a sample of low-redshift clusters. Asterisks indicate clusters considered as having a strong cooling flow. The numbers in column 6 indicate the references from which the luminosity and the temperature, respectively, are taken ( $\Omega_0 = 1$  and  $H_0 = 50$  km/s/Mpc). The quoted error bars are given at the 90% confidence level.

Cluster	$z$	$T_X$ keV	$L_{bol}$ $10^{44}$ erg/s	Ref.
Virgo	0.0038	$2.34^{+0.02}_{-0.02}$	0.68	28
Centaurus	0.01	$3.9^{+0.2}_{-0.20}$	1.22	1
A1060	0.0114	$3.1^{+0.3}_{-0.5}$	0.658	22
A262	0.0164	$2.4^{+0.3}_{-2.20}$	0.85	1
AWM7	0.0176	$4.0^{+0.3}_{-0.20}$	2.76	1
A426	0.0183	$6.3^{+0.3}_{-0.3}$	23.1	1
A539	0.0205	$3.0^{+0.8}_{-0.6}$	0.64	1
A1367	0.0215	$3.5^{+0.18}_{-0.18}$	2.2	1
3C 129	0.0218	$6.2^{+0.8}_{-0.6}$	3.7	1
A1656	0.0232	$8.11^{+0.07}_{-0.07}$	17.2	1
Ophiucus	0.028	$9.8^{+0.7}_{-0.3}$	27.4	22
A2199	0.0299	$4.5^{+0.3}_{-0.2}$	6.4	1
A496	0.032	$3.91^{+0.06}_{-0.06}$	7.16	1
A576	0.0381	$4.3^{+0.5}_{-0.4}$	2.94	1
A3558	0.048	$5.5^{+0.3}_{-0.2}$	10.	1,8
Triangulum	0.051	$10.3^{+0.8}_{-0.8}$	30.	12
A85	0.052	$6.2^{+0.4}_{-0.5}$	15.8	1
A3667	0.053	$6.5^{+0.8}_{-0.99}$	21.4	15
A754	0.0534	$8.5^{+0.82}_{-0.82}$	29.4	26
A2319	0.0564	$10.0^{+0.7}_{-0.7}$	37.	11
A2256	0.0601	$7.51^{+0.19}_{-0.19}$	24.3	1
A1795	0.0616	$6.7^{+0.66}_{-0.66}$	23.75*	16
A399	0.07	$7.0^{+1.0}_{-1.0}$	14.2	5
A644	0.0704	$6.6^{+0.17}_{-0.17}$	23.5	1
A401	0.0748	$8.0^{+1.0}_{-1.0}$	30.8	5
A2142	0.0899	$9.0^{+0.2}_{-0.2}$	56*	30

### 2.1. Measuring $\Omega_0$ with clusters

OB97 and OBB97 have used the observed correlation  $L_X - T_X$  to construct a self-consistent modeling of X-ray clusters. The relation between luminosity and temperature they used is:

$$L_{bol} = L_1 T_{keV}^\alpha \quad (1)$$

with  $L_1 = 0.049 \cdot 10^{44}$  erg/s and  $\alpha = 3$ . A more recent analysis (Arnaud & Evrard, 1997) showed that the  $L_X - T_X$  does have a moderate intrinsic dispersion when cooling flow clusters are removed, with  $L_1 = 0.067 \cdot 10^{44}$  erg/s and  $\alpha = 2.89$ . By comparing to the EMSS cluster redshift distribution, OB97 have shown that in the absence of evolution of the  $L_X - T_X$  relation, open models with  $\Omega_0 \sim 0.2$  predict much more clusters than observed while  $\Omega_0 = 1$  model fits the data reasonably well, although the abundance of high redshift clusters was not very well reproduced.

They have investigated the possibility of evolution by allowing the relation  $L_X - T_X$  to change with redshift according to the following form:

$$L_{bol} = L_1 (1 + z)^\beta T_{keV}^\alpha \quad (2)$$

where  $\beta$  is a free parameter which can be derived by fitting the redshift distribution of the cluster EMSS survey. They found that  $\beta = 1$  for a flat universe ( $\Omega_0 = 1$ ), corresponding to positive evolution, while a significant negative evolution, corresponding to  $\beta = -2.3$  was required for an open universe ( $\Omega_0 \sim 0.2$ ). Following a similar approach and by fitting the ROSAT number counts, Kitayama & Suto (1997) provided constraints on the parameters of the model and Mathiesen & Evrard (1997) reached essentially identical conclusions. Kitayama et al. (1997) has extended the predictions to the SZ counts. The self-similar model predicts  $\alpha = 2.0$  and  $\beta = 1.5$ , but  $\alpha = 2.0$  is clearly ruled out by observations, and physical processes specific to the baryonic content have to be advocated. For instance, HA91 assumed an isentropic model. Bower (1997) has recently re-examined this question in more detail.

### 3. The high-redshift cluster sample

In order to perform this new cosmological test, we have collected from the literature all the information on temperature measurements of X-ray clusters. Although the number of high redshift clusters ( $z > 0.4$ ) with an estimation of the X-ray temperature remains small, ASCA observations of clusters of relatively high redshift ( $z \approx 0.3$ ) has begun to appear in the literature. We have tried to compile all the existing X-ray clusters with redshift greater than 0.15 for which the temperature has been measured with various X-ray satellites, mostly ASCA. This represents 56 clusters whose properties are summarized in Table 2.

In order to address the question of the possible evolution of clusters, we have decided to include some clusters for which a reliable mass estimate is available and derived the corresponding temperature. This has led us to include the CNOC survey of clusters by C97, as it contains accurate velocity dispersion measurements, and the sample of Smail et al. (1997) (hereafter S97), who have used deep HST images to study weak shear of background galaxies by distant clusters of galaxies to estimate their masses. From these two samples, only clusters for which temperature information was not available were retained in the analysis. The final compilation contains a total number of 65 clusters at high redshift ( $z > 0.15$ ), 32 being at redshift greater than 0.3. The most distant redshift clusters of the sample are MS1054.5-0321 at  $z = 0.83$  which has been measured by Donahue et al. (1997) and AXJ2019 at  $z = 1$  by Hattori et al. (1997). An additional list of clusters at low redshift, for which accurate temperature information was available, has been added to the sample for the purpose of our analysis, but we do not attempt to be complete. This set is used as a template (Table 1).

Ideally, in order to perform the cosmological test, it would be better to estimate the evolution of  $L_X - T_X$  from the EMSS sample itself. However, too few measurements exist up to now. Still, our sample contains a number of high redshift clusters which is comparable to that of the EMSS sample in the various redshift ranges. For comparison, the EMSS survey (Gioia & Luppino 1984) has the same number of clusters at  $z > 0.3$  but a total number of  $z > 0.15$  of only 49 (Fig. 1). This is important as it does mean that we are testing the evolution of the  $L_X - T_X$

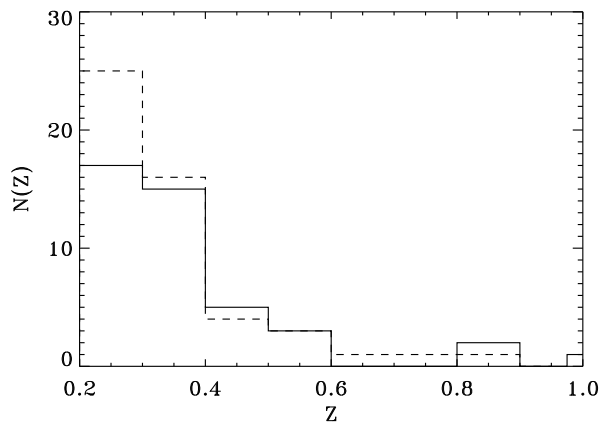


**Fig. 1.** The redshift distribution of X-ray clusters in our sample (full line) compared with the one in the EMSS cluster survey (hashed line).

relation over the same redshift range as OB97 have investigated, with a similar number of clusters involved.

#### 3.1. Fluxes

As the available data come from different satellites, the published luminosities are given in various energy bands. Therefore, when the bolometric luminosity was not available, it has been estimated by using a Raymond-Smith code, taking an average metallicity of 0.33 when its value was not available (see Tables 1, 2). Flux calibration is a serious worry when data from different satellites are used. Arnaud & Evrard (1997) have shown that GINGA and ROSAT fluxes agree very well, while an offset in the calibration of EXOSAT is suspected. In some cases, several flux estimates are given, which disagree from time to time. Our fluxes were taken from different authors: David et al. (1991), Mushotzky & Scharf (1997) (hereafter M&S97), Ebeling (1996) from ROSAT PSPC observations and Nichol *et al.* (1997) from HRI observations. In general, we have preferred ROSAT measurements when available.

#### 3.2. Cooling flows

Cooling flow clusters present a central enhancement in their luminosity, in a region where the cooling time of the gas is shorter than the Hubble time. The inclusion of such clusters in our analysis is problematic: as they are more luminous than “normal clusters”, they might introduce a bias. However, as the EMSS is flux selected, there is no reason to assume that cooling flow clusters are not present in the EMSS sample as well. Their point-like nature could even represent a bias favoring their presence in the EMSS, as the high background makes the detection of extended source more difficult. Still, it is also conceivable that cooling flow clusters are overabundant in the general compilation compared to the EMSS sample. We have therefore applied a correction to clusters for which the presence of a cooling flow was known: only the flux outside the cooling flow was taken into account. Such cooling flow clusters are flagged by an asterisk.

**Table 2.** X-ray temperatures and bolometric luminosities for high redshift clusters.

Cluster	$z$	$T_X$ keV	$L_{bol}$ $10^{44} \text{erg/s}$	Ref.	Cluster	$z$	$T_X$ keV	$L_{bol}$ $10^{44} \text{erg/s}$	Ref.	
A2204	0.153	$8.5^{+0.4}_{-0.45}$	76.	2	A483	0.28	$8.7^{+3.3}_{-2.2}$	48.9	1	
A3888	0.168	$7.9^{+0.3}_{-1.0}$	33.	17	A1758N	0.28	$10.2^{+2.3}_{-1.7}$	29.	6,2	
A1204	0.17	$3.6^{+0.13}_{-0.13}$	14.	18	Zw3146	0.291	$6.2^{+1.2}_{-0.7}$	64.*	7	
A586	0.171	$6.8^{+0.7}_{-0.67}$	17.96	3	A1722	0.301	$5.87^{+0.51}_{-0.41}$	21.	2	
RXJ 1340+4018	0.171	$0.92^{+0.13}_{-0.13}$	0.45	27	MS1147.3	0.303	$5.5^{+1.32}_{-1.00}$	6.6	32	
A2218	0.175	$6.72^{+0.83}_{-0.83}$	19.3	1	MS1008	0.306	$7.9^{+2.00}_{-1.65}$	16.32	32	
A1689	0.181	$8.7^{+0.51}_{-0.49}$	47.9	3	AC118	0.308	$9.33^{+1.09}_{-0.83}$	48.	3	
A665	0.182	$8.9^{+0.62}_{-0.61}$	28.	3	MS1241.5	0.312	$6.2^{+3.00}_{-2.15}$	6.4	32	
A1763	0.187	$9.0^{+1.02}_{-0.84}$	35.5	6,2	MS0811.6	0.312	$4.6^{+1.50}_{-1.00}$	4.76	32	
A1246	0.187	$6.3^{+0.54}_{-0.51}$	19.5	2	MS2137	0.313	$4.7^{+0.5}_{-0.3}$	34.19	32	
SC 2059-25	0.188	$7.0^{+6.9}_{-2.2}$	23.15	9	A1995	0.318	$9.44^{+2.18}_{-1.54}$	22.5	3	
MS0839.8	0.194	$3.8^{+0.4}_{-0.31}$	7.4	3	MS0353	0.32	$6.2^{+1.65}_{-1.32}$	12.85	32	
A2507	0.196	$9.4^{+2.7}_{-1.9}$	40.	1	MS1426.4	0.32	$5.5^{+1.82}_{-1.15}$	8.85	32	
MS0440	0.1965	$5.6^{+0.80}_{-0.60}$	6.1	31,19	MS1224.7	0.326	$4.3^{+1.15}_{-1.00}$	7.46	32	
A2163	0.201	$14.6^{+0.9}_{-0.80}$	143.	13	MS1358	0.329	$6.6^{+0.82}_{-0.82}$	18.94	32	
A520(MS0451+02)	0.201	$8.6^{+0.93}_{-0.90}$	17.	4,2	A959	0.353	$6.47^{+1.15}_{-1.01}$	16.	3	
A963	0.206	$6.76^{+0.44}_{-0.49}$	21.	2	MS1512	0.3726	$3.8^{+0.66}_{-0.50}$	8.212	32	
A1851	0.2143	$5.04^{+0.8}_{-0.68}$	6.23	3	A370	0.373	$6.39^{+1.02}_{-0.81}$	21.7	3	
A773	0.217	$9.6^{+1.03}_{-0.90}$	30.	6,2	A851	0.41	$6.7^{+2.7}_{-1.70}$	15.	2	
A1704	0.219	$4.5^{+0.56}_{-0.34}$	13.	2	CI 09104+4109	0.442	$11.4^{+3.2}_{-3.2}$	75.	20	
A1895	0.225	$6.7^{+1.38}_{-1.05}$	10.5	3	RXJ1347.5-1145	0.451	$9.3^{+1.1}_{-1.0}$	210.*	23	
A2390	0.228	$8.9^{+0.97}_{-0.77}$	54.	2	3C295	0.46	$7.13^{+2.06}_{-1.35}$	24.	2	
A2219	0.23	$11.8^{+1.26}_{-0.74}$	57.	6,2	MS0451-03	0.5392	$10.4^{+1.60}_{-1.30}$	46.8	24	
MS1305.4	0.241	$2.98^{+0.52}_{-0.41}$	2.86	2	RXJ 0018.8+160	0.544	$1.6^{+0.7}_{-0.4}$	0.6	3.2	29
A1835	0.252	$9.1^{+2.10}_{-1.30}$	80.*	7	CL0016+16	0.5466	$7.55^{+1.188}_{-0.957}$	55.	10	
Zw 7160	0.258	$5.2^{+2.2}_{-0.70}$	30.*	7	RXJ1716+67	0.813	$6.7^{+2.0}_{-2.0}$	17.72	33	
A348	0.274	$4.85^{+0.6}_{-0.6}$	3.6	36	MS1054.5-0321	0.826	$14.7^{+4.6}_{-3.5}$	42.	25	
A33	0.28	$4.06^{+0.5}_{-0.5}$	2.4	36	AXJ2019	1.0	$8.6^{+6.9}_{-4.9}$	19	35	

**Ref.** (1) David et al., 1993; (2) Mushotzky & Scharf, 1997; (3) Tsuru et al., 1996; (4) Nichol et al., 1997; (5) Fujita et al. 1997; (6) Ebeling et al. 1995; (7) Allen et al. 1995; (8) Markevitch & Vikhlinin, 1997; (9) Arnaud et al., 1991; (10) Hughes & Birkinshaw, 1997; (11) Markevitch, 1996; (12) Markevitch et al., 1996; (13) Elbaz et al., 1996; (14) Tamura et al., 1996; (15) Knopp et al., 1996; (16) Briel & Henry, 1996; (17) White & Fabian, 1996; (18) Matsuura et al., 1996; (19) Gioia private communication; (20) Hall et al., 1996; (21) Hamana et al., 1997; (22) Matsuzawa, et al., 1996; (23) Schindler et al., 1996; (24) Donahue, 1996; (25) Donahue, et al., 1997; (26) Henriksen & Markevitch, 1996; (27) T.J. Ponman et al., 1994; (28) Arnaud & Evrard, 1997; (29) Connolly et al., 1996; (30) White et al., 1994; (31) Gioia & Luppino, 1994; (32) Henry 1997; (33) Henry & Gioia 1997; (34) Schindler, 1997; (35) Hattori et al., 1997; (36) Colafrancesco, 1997;

In practice, this correction is never larger than 50%. This has been applied only to a few number of clusters.

### 3.3. Deriving the temperature

As explained in Sect. 3, our sample is not based on clusters with measured temperature only: it also contains distant clusters for which the temperature information has been estimated in an indirect way. From the lensing analysis, S97 have used deep WFPC-2 imaging of 12 distant clusters at redshifts between  $z = 0.17$  and  $0.56$ . Using the distortion of faint galaxies detected in these fields, they measured the mean shear and inferred a mass estimate within a radius of  $200h^{-1}$  kpc from the cluster lens center, assuming a singular isothermal profile  $\propto r^{-2}$ . We have used these masses to derive the X-ray temperature of these 11 distant clusters, applying the following scaling

relation:

$$T_X = 5.38 M_{lens} \text{keV} \quad (3)$$

where  $M_{lens}$  is in units of  $10^{14} h^{-1} M_{\odot}$ . For the C97 clusters, we have converted the virial masses derived inside the total radial extent of the sample from the measured velocity dispersions to an X-ray temperature. For this, we used the scaling relations derived from Evrard's numerical simulations (Evrard 1989, Evrard 1997), we infer a relation between velocity dispersion and temperature:

$$T_X = (\sigma/350 \text{km/s})^2 \text{keV} \quad (4)$$

In some cases, it has been possible to compare the temperature as estimated from (3) and (4) with satellite temperature measurements (see Tables 3 and 4).

Although the number of clusters for which the information is available is small, the agreement is rather good (Fig. 2). This

**Table 3.** Comparison between virial temperatures estimated from the velocity dispersion  $\sigma$  (CNO Survey C97) with measured temperatures: <sup>a</sup>M&S97; <sup>b</sup>Gioia 1997; <sup>c</sup>Henry 1997; <sup>d</sup>Donahue 1996; <sup>e</sup>Tsuru et al. 1997; <sup>f</sup>Allen et al. 1995.

Cluster	$z$	$\sigma$ km/s	$T_{est}$ keV	$T_X$ keV
A2390	0.228	1104	9.95	8.9 <sup>a</sup>
MS0440	0.1965	606	3.00	5.6 <sup>b</sup>
MS1008	0.306	1054	9.07	7.9 <sup>c</sup>
MS1358	0.329	934	7.12	6.6 <sup>c</sup>
MS1512	0.373	690	3.88	3.8 <sup>c</sup>
MS0451+02	0.2011	1031	8.70	8.6 <sup>a</sup>
MS0451-03	0.5392	1371	15.30	10.4 <sup>d</sup>
MS0839	0.1928	756	4.66	3.8 <sup>e</sup>
MS1455(Zw 7160)	0.258	1133	10.50	5.2 <sup>f</sup>
MS1224	0.3255	802	5.2	4.3 <sup>c</sup>

**Table 4.** Comparison between estimated temperatures from  $M_{lens}$  (weak lensing, S97) with measured temperatures: <sup>a</sup>David et al. 1993; <sup>b</sup>Tsuru et al. 1997; <sup>c</sup>Hughes & Birkinshaw, 1997; <sup>d</sup>M&S97.

Cluster	$z$	$M_{lens}$ $10^{14}M_{\odot}$	$T_{est}$ keV	$T_X$ keV
A2218	0.17	1.05	5.65	6.72 <sup>a</sup>
AC118	0.31	1.85	9.92	9.33 <sup>b</sup>
CL0016	0.55	1.87	10.06	7.55 <sup>c</sup>
A851	0.41	0.73	3.93	6.7 <sup>d</sup>
3C295	0.46	2.35	12.64	7.13 <sup>d</sup>

suggests that lensing and the virial mass estimates are essentially in agreement with the X-ray mass at a level better than a factor of two, although one can notice a slight tendency towards overestimation, but the samples are too small to draw any firm conclusion.

## 4. Method and results

### 4.1. Investigating the possible evolution

Ideally, one would like to estimate directly the  $L_X - T_X$  in a redshift bin centered on a value of the redshift as high as possible. However, since the number of clusters decreases rapidly for redshifts greater than 0.25, it becomes difficult to get any information from this method at high redshift: dividing the sample in several redshift bins and trying to fit the luminosity-temperature relation in the different redshift bins becomes unpractical for redshifts greater than 0.35. Another method has been used which consists in plotting the mean temperature of clusters above some threshold luminosity in order to minimize any possible systematic effect (Arnaud et al, 1991, M&S97). It remains possible, however, that higher redshift clusters are brighter in the mean, introducing a bias in the sample. Furthermore, this method results in a rude elimination of some of the data. We have tried to find an efficient estimator of the evolution which is adequate for the kind of evolution introduced by OB97. To get round this problem we have introduced a new evolution estimator. For each

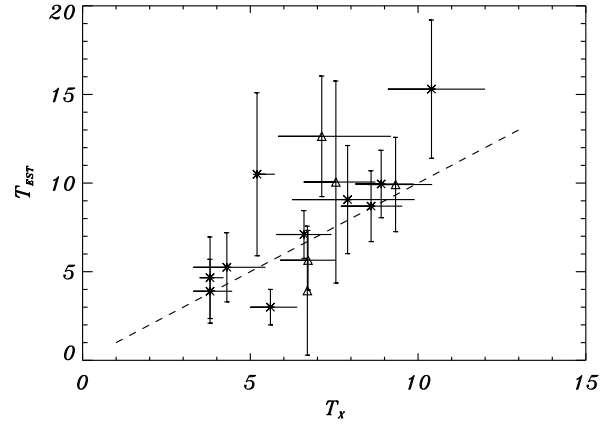


**Fig. 2.** Comparison between estimated temperatures  $T_{est}$  from  $M_{lens}$  as inferred from weak lensing S97 (triangles) and from CNO survey velocity dispersions (crosses) with measured temperatures  $T_X$ . Error bars are at 90% confidence level.

cluster  $i$ , with measured  $L_i, T_i$ , we have estimated the following quantity:

$$C_i = \frac{L_i}{L_1 T_i^\alpha} \quad (5)$$

where  $L_1 = 0.04910^{44}$  erg/s and  $\alpha = 3$ . The dependance of  $C_i$  on redshift probes the evolution: clearly, if the cluster population is not evolving, the mean value of this quantity should remain constant with redshift. Note that it is possible that the  $L_X - T_X$  evolves and that the measured  $C$  will not probe this evolution, this would need, however, some kind of conspiracy. Because  $L_X$  is estimated from the apparent flux,  $C(z)$  also contains a term coming from the cosmological parameters of the universe in the luminosity distance. In practice,  $L_X$  is estimated in a Einstein-de Sitter universe; therefore, the theoretical value  $C(z)$  has to be corrected when one is comparing data with low-density universe predictions (however, this term is small, as can be seen in Fig. 3). It is also clear that this method can be applied without removing any data, and that it takes fully taking into account the information in redshift. We have applied this test to our sample using the OB97 parameters for the  $L_X - T_X$  relation. For each cluster, we have computed the quantity given by (5) and estimated an uncertainty range on this quantity, neglecting the uncertainty in the luminosity. The result is plotted in Fig. 4.1.

The measure of evolution can now be directly obtained by fitting a power law to the data:

$$C(z) = \alpha(1+z)^\beta \quad (6)$$

in which  $\alpha$  and  $\beta$  are determined by a likelihood analysis. However, the intrinsic dispersion of the values of  $C$  is often higher than the uncertainty on the coefficient itself, due to the errors in the temperature. We have therefore estimated the intrinsic dispersion of  $C$  from our template sample and added it in quadrature with the uncertainty on the individual values of the coefficient. We have also checked that the results are insensitive to

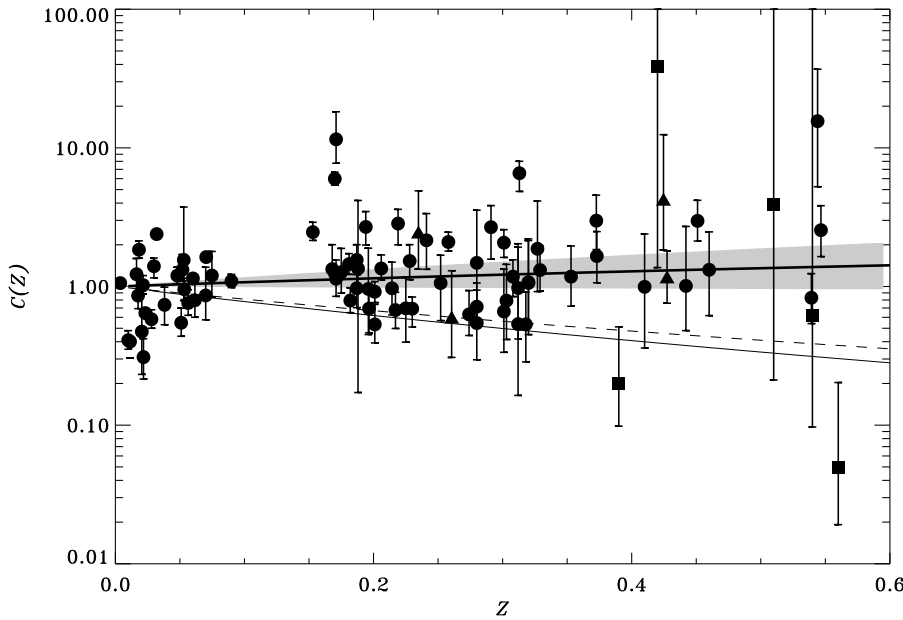


**Fig. 3.** In this figure we present the coefficient  $C_i$  for all the clusters in our sample with redshift smaller than 0.6. The filled circles are used for actual X-ray measurement of the temperature, filled squares are for weak lensing measurements of S97 and filled triangles are for the CNOC clusters. The error bars are  $1\sigma$ . The thick line represents the best fitting power-law, the shaded area represents an estimate of the 90% confidence range. The prediction of a low density universe ( $\Omega_0 = 0.2$ ) is represented by the thin line. The dashed, thin line is the curve when the correction in the luminosity distance is not taken into account in the expression of  $C(z)$ .

the assumed dispersion. In order to investigate the robustness of our results, we have performed various analyses, whose results are summarized in Table 5: for various sub-samples, we have reported the best estimated parameters from the likelihood analysis and the 68% and 90% confidence limits. The expected value of  $\alpha$  is 1. If only clusters with redshift greater than 0.15 are used, there is a degeneracy between  $\alpha$  and  $\beta$ : in the two-parameter plane, the confidence domain looks like an elongated ellipse, allowing a wide range of  $\beta$ , but for unrealistic values of  $\alpha$ . This is the main motivation to include a set of low redshift clusters in our sample, before performing the likelihood analysis. With this approach,  $\alpha = 1$  value always falls in the 90% confidence range when  $\alpha$  and  $\beta$  are determined by a likelihood analysis. In our analysis, we have generally assumed a gaussian distribution of the errors, which is equivalent to a  $\chi^2$  minimization. When the full sample is used, the  $\chi^2$  of the best fitting model is rather poor:  $\chi^2$  is equal to 219 for 97 clusters. This is due to a few outliers, which are far away from the general trend. This can be seen by using the  $l_1$  norm instead of the standard  $\chi^2$ . Four clusters were found to have high  $C$  value (A1204, RXJ 1340+4018, MS2137, RXJ 0018+16) and were removed in most sub-samples (in this case the sub-sample is flagged by -o in Table 5).

The X-ray data, even when they are split into various sub-samples (like the EMSS X-ray clusters alone or the Henry set alone) always lead to a high value of the best  $\beta$ , in the range  $[0. - 1.0]$ . It is important to note that no systematic trend is found: the various X-ray selected samples always give a  $\beta$  in the same range, with an uncertainty at worst of the order of 0.5. Therefore the range  $[0. - 1.0]$  can be taken as the 90% confidence interval. The only two samples which do not lead to a high value of  $\beta$  are the CNOC sample and the S97 sample with their estimated temperatures (from virial and lensing mass estimates). However, when these samples are restricted to clusters for which the temperature has been measured (the X-ray CNOC and X-ray S97 sample in Table 3), the resulting  $\beta$

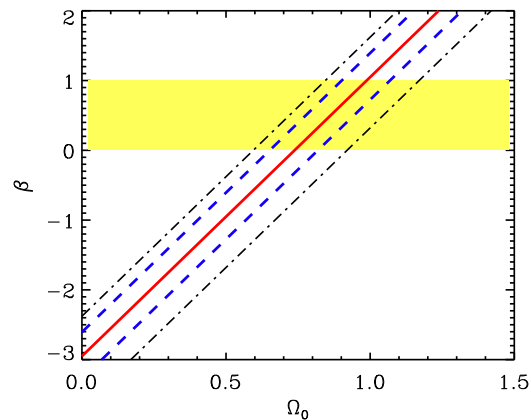


**Fig. 4.** Comparison of the predicted values of the coefficient to the values we have estimated from the observations. The grey area corresponds to our 90% confidence range for  $\beta$ . The solid thick line corresponds to the best evolution law when the EMSS redshift distribution is fitted, the dashed (resp. dotted-dashed) correspond to an estimation of the 68% contour (95% resp.).

is much higher and in agreement with other analysis based on X-ray data. This may be due to the fact that lensing and virial mass estimates are higher than X-ray masses, which introduces a bias toward lower  $C$  and, consequently, to artificially lower  $\beta$  at high  $z$ . Our result confirms previous investigations: available data on X-ray clusters are consistent with the lack of significant evolution in the  $L_X - T_X$  relation. Finally, it is somewhat troublesome that the highest redshift clusters ( $Z > 0.8$ ) lead to a small value of  $C$ . Better temperature and flux measurements will be of great interest, and we obviously need more (very) high redshift clusters temperature measurements.

**Table 5.** This table summarises the main results of the various fits we have performed. The full sample with 56 X-ray clusters with measured X-ray temperatures plus 4 CNOC clusters and 5 S97 clusters for which the temperature is derived from the virial velocity dispersion and lensing mass respectively. Col. 2 gives the number of high redshift clusters ( $z > 0.15$ ), the  $\delta\chi^2$  value in col. 3 (the contribution of the low redshift cluster subset to the  $\chi^2$  is nearly constant and equal to 26.), the best fit estimates of  $\alpha$  and  $\beta$  with the uncertainties at 68% and 90% confidence level are given in col. 4 and col. 5 respectively and the corresponding value of  $\Omega_0$  as inferred from Eq. 7 and the 90% uncertainties are given in col. 6.

Sub-sample	$N_c$	$\delta\chi^2$	$\alpha \pm 68\% \pm 90\%$	$\beta \pm 68\% \pm 90\%$	$\Omega_0 \pm 90\%$
Complete sample	65	193.	$1.15^{+0.10+0.20}_{-0.10-0.15}$	$0.00^{+0.30+0.50}_{-0.30-0.60}$	$0.75^{+0.12}_{-0.15}$
( $L_1$ norm)	65	63.	$1.05^{+0.15+0.25}_{-0.15-0.25}$	$-0.10^{+0.60+1.00}_{-0.60-1.10}$	$0.72^{+0.25}_{-0.27}$
X-ray sample	56	182.	$1.14^{+0.10+0.15}_{-0.10-0.15}$	$+0.28^{+0.30+0.50}_{-0.35-0.60}$	$0.82^{+0.15}_{-0.17}$
	56	184.	<b>1.00</b>	$+0.65^{+0.25+0.35}_{-0.20-0.35}$	$0.91^{+0.09}_{-0.09}$
X-ray sample -o	52	68.	$1.07^{+0.10+0.17}_{-0.05-0.13}$	$+0.20^{+0.30+0.60}_{-0.35-0.70}$	$0.80^{+0.15}_{-0.17}$
	52	69.	<b>1.00</b>	$+0.40^{+0.20+0.40}_{-0.30-0.50}$	$0.85^{+0.10}_{-0.12}$
X-ray sample $0.15 < z < 0.6$ -o	49	62.	$0.98^{+0.10+0.17}_{-0.10-0.15}$	$+0.95^{+0.35+0.65}_{-0.40-0.75}$	$0.99^{+0.16}_{-0.19}$
	49	62.	<b>1.00</b>	$+0.82^{+0.35+0.45}_{-0.25-0.50}$	$0.95^{+0.11}_{-0.12}$
X-ray sample $0.15 < z < 0.35$ -o	41	49.	$1.00^{+0.12+0.18}_{-0.10-0.18}$	$+0.65^{+0.50+1.00}_{-0.65-1.05}$	$0.92^{+0.25}_{-0.26}$
	41	49.	<b>1.00</b>	$+0.65^{+0.35+0.55}_{-0.35-0.60}$	$0.92^{+0.14}_{-0.15}$
X-ray sample $0.35 < z < 0.6$ -o	8	11.	$0.95^{+0.10+0.17}_{-0.10-0.17}$	$+1.30^{+0.45+0.75}_{-0.60-1.05}$	$1.07^{+0.20}_{-0.25}$
	8	11.	<b>1.00</b>	$+1.10^{+0.40+0.60}_{-0.55-0.80}$	$1.02^{+0.15}_{-0.20}$
EMSS	16	52.	$1.00^{+0.12+0.20}_{-0.08-0.15}$	$+0.00^{+0.50+0.80}_{-0.60-1.10}$	$0.75^{+0.20}_{-0.27}$
	16	52.	<b>1.00</b>	$+0.10^{+0.30+0.60}_{-0.40-0.80}$	$0.77^{+0.15}_{-0.20}$
EMSS $z < 0.6$ -o	14	11.6	$0.95^{+0.12+0.20}_{-0.10-0.15}$	$+0.25^{+0.75+1.00}_{-0.75-1.35}$	$0.81^{+0.25}_{-0.34}$
	14	11.7	<b>1.00</b>	$+0.15^{+0.50+0.80}_{-0.55-1.05}$	$0.79^{+0.20}_{-0.26}$
Henry -o	9	7.5	$0.95^{+0.10+0.20}_{-0.10-0.17}$	$+0.60^{+0.80+1.40}_{-1.00-1.75}$	$0.90^{+0.35}_{-0.40}$
	9	7.6	<b>1.00</b>	$+0.40^{+0.60+0.95}_{-0.70-1.20}$	$0.85^{+0.24}_{-0.30}$
CNOC ( $T_{est}$ )	15	2.	$1.05^{+0.10+0.20}_{-0.15-0.20}$	$-1.50^{+1.30+2.10}_{-1.50-3.30}$	$0.37^{+0.50}_{-0.82}$
X-ray CNOC ( $T_X$ )	10	18.	$0.95^{+0.10+0.20}_{-0.10-0.15}$	$+1.20^{+0.50+0.90}_{-0.70-1.20}$	$1.05^{+0.22}_{-0.30}$
Smail sample ( $T_{est}$ )	10	3.3	$1.05^{+0.15+0.25}_{-0.10-0.20}$	$-2.00^{+1.00+1.50}_{-1.70-3.00}$	$0.25^{+0.40}_{-0.75}$
X-ray Smail sample ( $T_X$ )	5	4.	$0.95^{+0.10+0.17}_{-0.12-0.18}$	$+1.20^{+0.70+1.10}_{-0.75-1.40}$	$1.05^{+0.28}_{-0.35}$
X-ray Smail sample ( $T_{est}$ )	5	2.	$1.05^{+0.15+0.20}_{-0.10-0.15}$	$+0.90^{+1.30+1.90}_{-1.60-2.60}$	$0.52^{+0.48}_{-0.65}$

#### 4.2. What do the data tell us?

As discussed previously, the knowledge of the evolution of the number density of clusters with redshift is a powerful cosmological test. By fitting the EMSS cluster redshift distribution, OB97 showed that the knowledge of evolution of the temperature-luminosity relation provides an alternative way to measure the mean density of the universe. We have iterated OB97 analysis for various values of the density parameter: the temperature distribution  $N(T_X)$  was fitted in order to derive the power spectrum index of the fluctuations as well as its normalization; the best  $\beta$  in Eq. (2) was then determined by fitting the EMSS redshift distribution, as well as the 1- and 2- sigma interval. The best fitting parameter  $\beta$  is tightly related to  $\Omega_0$  accordingly to the following relation:

$$\beta = 4. \times \Omega_0 - 3. \quad (7)$$

This relation, as well as the 1- and 2- sigma interval contours, are presented on Fig. 4. The high value of the slope illustrates the strong dependence on  $\Omega_0$ , highlighting the power of this test.

From the range of  $\beta$  we estimated from the data, we can obtain an estimation of  $\Omega_0$ . This is presented in Fig. 4, where we have plotted the value of  $\beta$  which is necessary to fit the EMSS cluster redshift distribution as well as the confidence range. The grey area represents the range  $[0. - 1.]$ , which is used as our 90% range obtained from the likelihood analysis. As one can see, the range of values we obtained favors a high density universe with a formal determination of the mean density parameter:  $\Omega_0 = 0.85^{+0.2}_{-0.2}$ . The main potential problem in our analysis is that the correspondence between  $\beta$  and  $\Omega_0$  has been obtained by OB97 from the EMSS survey, while the sample we used consists of clusters for which selection rules cannot be defined in a simple way. There are some limitations in the present work which imply that the conclusion should be considered as only preliminary: firstly, because the selection function of X-ray clusters in EMSS is not well understood, it is conceiv-

able that a substantial number of clusters have been missed (for instance because their surface brightness was too low). This is not supported by the fact that the modeling of X-ray clusters as done by OB97 predicted correctly the abundance of faint clusters as detected by ROSAT. Secondly, it is possible that our sample contains clusters which have preferentially high  $\beta$  as we have already mentioned; it is possible that these clusters suffer from a systematic bias favoring high  $\beta$ . Still, we do not find any evidence of such a bias. For instance, the typical luminosity in the sample does not seem to increase with redshift. In general, no systematic tendency was found by eye inspection. Thirdly, OB97 normalized the models at  $z = 0$  by use of the HA91 temperature distribution function, which may suffer from systematic uncertainties (Eke et al., 1996, Henry, 1997). A more detailed investigation of these various questions would need a Monte-Carlo simulation as well as a systematic investigation of possible biases. This will be addressed in a future paper.

## 5. Conclusion and discussion

In this paper, we have addressed the question of the cosmological evolution of the  $L_X - T_X$  relation and we have investigated the possible cosmological implications of this evolution (or lack of it). The new indicator  $C(z)$  is well adapted to measure the possible evolution of the  $L_X - T_X$  relation when the number of available clusters is small. We have applied this measure to a sample of high and intermediate redshift clusters for which the temperature information is available. We have found no strong evidence of evolution of the  $L_X - T_X$  relation, in agreement with other works. Despite the fact that our sample is not complete and that the number of high redshift clusters is not large, we have shown that our method is robust and leads to statistically significant result. We have furthermore used our results on  $L_X - T_X$  evolution to constrain the value of  $\Omega_0$  accordingly to the test of OB97. This is indeed the first time that this test is applied to observations. This test is extremely powerful because it results from a fundamental difference between high- and low-density universes: the rate of structure formation. Therefore, it provides a global test of the mean density of the universe, rather than a local dynamical one, as are classical  $M/L$  estimates. One can therefore expect to obtain in this way a definitive answer on the value of the mean density of the universe.

The absence of negative evolution in the  $L_X - T_X$  relation, as we have found, provides an indication of a high-density universe: accordingly to our analysis, the range of evolution we find is consistent with  $\Omega_0 = 0.85^{+0.2}_{-0.2}$  (at 90% confidence level). The fact that our sample is not drawn from an X-ray selected sample implies a possible bias and therefore our conclusion can be considered as only preliminary. A more robust answer on the mean density of the universe can be obtained only from a well-controlled X-ray selected sample of clusters. Our work shows that even if no definitive conclusion can be drawn, a reasonable number of X-ray temperature measurements can provide a very interesting answer on the mean density of the universe and that open model universes seem to be facing a serious problem. It is interesting to note that Barbosa et al. (1996) have also pointed

out an other piece of evidence coming from clusters which disfavors open model universes. It is realistic to envisage that a definitive answer could be obtained with XMM by a follow-up of a sample of high redshift clusters selected from an X-ray flux limited survey.

*Acknowledgements.* We acknowledge useful discussions with M. Arnaud and J. Bartlett, as well as the referee, A. Evrard, whose comments helped to improve this paper. We also thank Jens Hjorth for comments.

## References

- Allen, S.W., Fabian, A.C., Edge, A.C., Bautz, M.W., Furuzawa, A. & Tamara, Y. 1996, MNRAS, 283, 263
- Allen, S.W., Fabian, A.C. & Kneib, J.P. 1995, MNRAS, 279., 615
- Arnaud, M., Lachièze-rey, M., Rothenflug, R., Yamashita K. & Hatsu-kade, I. 1991, A&A, 243, 56
- Arnaud, M. & Evrard, A.E. 1997, in preparation
- Bahcall, N. A., Fan, X. & R. Cen 1997, ApJ, 485, L53
- Balland, C. & Blanchard, A. 1997, ApJ, 487, 33
- Barbosa D., Bartlett J.G., Blanchard A. & Oukbir J., 1996, A&A, 314, 13
- Bartlett, J.G., & Silk, J. 1993, ApJL, 407, L45
- Blanchard, A., Wachter, K., Evrard, A.E. & Silk, J. 1992, ApJ, 391, 1
- Bower, R.G. 1997, MNRAS in press, astro-ph/9701014
- Briel, U. & Henry, J.P. 1996, ApJ, 473, 131
- Carlberg, R.G., Morris, S.L., Yee, H.K.C. & Ellingson, E. 1997, ApJ, 479, L19
- Colafrancesco, S., & Vittorio, N. 1994, ApJ, 422, 443
- Colafrancesco, S. 1997, private communication.
- Collins C.A., Burke D.J., Romer A.K., Scharples R.M. & Nichol, R.C. 1997, ApJ 479, 117
- A. J. Connolly, A. S. Szalay, D. Koo, A. K. Romer, B. Holden, R. C. Nichol, & T. Miyaji 1997, ApJL, 473, L67
- David L. P., Slyz A., Jones C., Forman W., Vrtilek S. D. & Arnaud K. A. 1993, ApJ, 412, 479
- De Luca, A., Désert, F. X. & Puget, J. L. 1995, A&A, 300, 335
- Donahue, M. 1996, ApJ., 468, 79
- Donahue, M. et al., 1997, ApJ, submitted, astro-ph/9707010
- Ebeling, H., Vosges, W., Bohringer, H., Edge, A.C., Huchra, J. P. & Briel, U. G 1996, MNRAS, 281, 799
- Ebeling, H., Edge, A. C. Fabian, A. C., Allen, S. W. & Crawford, C. S. 1997, ApJ, 479, L101
- Edge, A., Stewart, G.C., Fabian, A.C. & Arnaud, K.A. 1991, MNRAS, 245, 559
- Edge, A. & Stewart, G., 1991, MNRAS, 252, 428
- Elbaz, D., Arnaud, M. & Bohringer, H., 1995, A&A, 293, 337
- Eke V. R., Cole S. & Frenk C. S. 1996, MNRAS, 282, 263
- Evrard, A.E., 1997, MNRAS, submitted, astro-ph/9701148
- Evrard, A.E. 1990, in Clusters of Galaxies, eds. W.R. Oegerle, M.J. Fitchett & L. Danly, (Cambridge Univ. Press.) p. 287
- Evrard, A.E., Metzler, C., Navarro, J.F. 1996, ApJ, 469, 494
- Fujita, Y., Koyama, K., Tsuru, T. & Matsumoto, H. 1997, PASJ, 48, 191
- Gioia, I.M. & Luppino, G.A. 1994, ApJS, 94, 583
- Hall, P.B., Ellingson, E. & Green, R.F. 1997, ApJ submitted
- Hamana, T. et al. 1997, preprint
- Hattori, M., et al. 1997, Nature, 388, 146
- Henriksen, M. J. & Markevitch, M. L. 1996, ApJ, 466, L79
- Henry, J. P & Arnaud, K. A. 1991, ApJ, 372, 410



- Henry, J. P., Gioia, I. M., Maccacaro, T., Morris, S. L., Stocke, J. T. & Wolter, A. 1992, *ApJ*, 386, 408
- Henry, J. P. 1997, *ApJL*, in press
- Hughes, J.P. & Birkinshaw, M. 1997, *ApJ*, submitted
- Kitayama, T. & Suto, Y. 1997, astro-ph/9702017
- Kitayama, T., Sasaki, S., Suto, Y. 1997, astro-ph/9708088
- Knopp G.P., Henry J.P & Briel U. 1996, *ApJ*, 472, 125
- Markevitch, M. 1996, *ApJL*, 465, 1
- Markevitch, M.L, Sarazin, Graig.L & Irwin, J.A. 1996, *ApJ*, 472, L17
- Markevitch, M. & Vikhlinin A. 1997, *ApJ*, 474, 841
- Mathiesen, B. & Evrard A. E. 1997, *MNRAS*, submitted, astro-ph/970376.
- Matsuura, M., Miyoshi, S.J., Yamashita, K., Tawara, Y., Furuzawa, A., Lasenby, A., Saunders, R., Jones, M., Hatsukade, I. 1996, *ApJ*, 466, L75
- Matsuzawa, H., Matsuoka, M., Ikebe, Y., Mihara T. & Yamashita, K. 1996, *PASJ*, 48, 565
- Mushotzky R. F. & Loewenstein M. 1997, *ApJ*, 481, L63
- Mushotzky R. F. & Scharf C. A. 1997, *ApJ*, 482, L13
- Nichol R. C., Holden B. P., Romer A. K., Ulmer M. P., Burke D. J., Collins C. A. 1997, *ApJ*, 481, 644
- Oukbir, J. & Blanchard A. 1992, *A&A*, 262, L21
- Oukbir, J. & Blanchard A. 1997, *A&A*, 317, 10
- Oukbir, J., Bartlett J.G. & Blanchard A. 1997, *A&A*, 320, 365
- Ponman, T.J., Allan, D.J., Jones, L.R., Merrifield, M., McHardy, I.M., Lehto, H.J. & Luppino, G.A. 1994, *Nature* 369, 462
- Press W.H. & Schechter P. 1974, *ApJ*, 187, 425
- Scharf, C., Jones, L. R., Ebeling, H., Perlman E., Malkan, M., & Wegner, G. 1997, *ApJ*, in press
- Smail, I., Ellis, R.S., Dressler, A., Couch, W.J, Oemler, A., Sharples, R.M., Butcher, H. 1997, *ApJ*, 479, 70
- Tamura, et al. 1996, *PASJ* 48, 671
- Tsuru, T., Koyama, K. Hughes, J., Arimoto, N., Kii, T. & Hattori, M. 1996, page 375 in *UV and X-ray Spectroscopy of Astrophysical and Laboratory Plasmas* edited by K. Yamashita & T. Watanabe, Universal Academy Press, Tokyo, Japan
- Viana, P. T. P., Liddle, A. R. 1996, *MNRAS*, 281, 323
- White, D.A. & Fabian, A.C. 1995, *MNRAS*, 273, 72
- White, R.E.III., Day, C.S.R., Hatsukade, I., Hughes J.P. 1994, *ApJ*, 433, 583